Epigenetics 7:10, 1188–1199; October 2012; © 2012 Landes Bioscience

Human-specific CpG "beacons" identify loci associated with human-specific traits and disease

Christopher G. Bell,[1,*] Gareth A. Wilson,[1] Lee M. Butcher,[1] Christian Roos,[2] Lutz Walter[2] and Stephan Beck[1,*]

[1]Medical Genomics; UCL Cancer Institute; University College London; London UK; [2]Gene Bank of Primates and Primate Genetics Laboratory; German Primate Centre; Leibniz Institute for Primate Research; Göttingen, Germany

Keywords: epigenetics, epigenomics, CpG islands, gene regulation, evolution, human disease

Abbreviations: BGC, biased gene conversion; CGI, CpG islands; MeDIP, methylated DNA immunoprecipitation; PBC, positive beacon clusters; PBMC, peripheral blood mononuclear cells

Regulatory change has long been hypothesized to drive the delineation of the human phenotype from other closely related primates. Here we provide evidence that CpG dinucleotides play a special role in this process. CpGs enable epigenome variability via DNA methylation, and this epigenetic mark functions as a regulatory mechanism. Therefore, species-specific CpGs may influence species-specific regulation. We report non-polymorphic species-specific CpG dinucleotides (termed "CpG beacons") as a distinct genomic feature associated with CpG island (CGI) evolution, human traits and disease. Using an inter-primate comparison, we identified 21 extreme CpG beacon clusters (≥ 20/kb peaks, empirical $p < 1.0 \times 10^{-3}$) in humans, which include associations with four monogenic developmental and neurological disease related genes (Benjamini-Hochberg corrected $p = 6.03 \times 10^{-3}$). We also demonstrate that beacon-mediated CpG density gain in CGIs correlates with reduced methylation in these species in orthologous CGIs over time, via human, chimpanzee and macaque MeDIP-seq. Therefore mapping into both the genomic and epigenomic space the identified CpG beacon clusters define points of intersection where a substantial two-way interaction between genetic sequence and epigenetic state has occurred. Taken together, our data support a model for CpG beacons to contribute to CGI evolution from genesis to tissue-specific to constitutively active CGIs.

Introduction

The CpG dinucleotide is unique for its ability to carry both genetic and epigenetic information in the genome of a differentiated mammalian cell.[1,2] Variation in DNA methylation, facilitated by this two base pair motif, influences gene expression, and thereby enables tissue-specific function.[3-6] However, this dinucleotide is substantially depleted, to one fifth of the expected level, due to the hypermutability (~11-fold) of cytosines when methylated.[7-9] Yet, a minority of CpGs is retained against this strong tide of loss by a variable combination of: evasion of methylation in the germline, functional importance or chance. These are predominantly in CpG dense regions.[10] Additionally, new CpGs are created by mutation through base substitution and as a by-product of the increase of GC in regions of biased gene conversion (BGC).[11]

A high density region of unmethylated CpGs can recruit CpG binding proteins, such as Cfp1 and KDM2A, which modify histone tails.[12,13] Thomson et al. have shown that the experimental inclusion of a cluster of unmethylated CpGs is sufficient to establish domains of H3K4me3.[12] This histone modification leads to genomic three-dimensional structure change and the acquisition of permissive chromatin regions within the expanse of repressed genome.[14] CpG clusters, termed CpG Islands (CGIs), co-locate with 60–70% of human gene promoters, often those of housekeeping genes that are hypomethylated in the germ line,[15,16] but also 40% that are tissue-specific.[10,17] Methylation of CGI promoters acts as a durable silencing mechanism. However, the majority of CGIs are unmethylated in differentiated cells independently of their transcriptional activity.[10,18] The methylation state of CGI is strongly correlated with its CpG content, with high density CGIs being predominately constitutively unmethylated and "weak" low density islands the preferred target for tissue-specific methylation.[10,19] CpG gain that shifts an island from weak to strong status therefore affects its dynamic ability for methylation change.

CpGs located in the lower density regions surrounding islands, termed CpG shores (~2 kb up- or down-stream), identify significant tissue-, cancer- and reprogramming-specific methylation variability.[6,20-22] Therefore, shore accretion and island erosion by subtle modulation in CpG density within these regions may have a disproportionate influence on the methylation levels and locations of these flanking regions. Additionally, an increase in methylation variance has been proposed to have an evolutionary important role, as well as being a potential influence on disease susceptibility.[23]

*Correspondence to: Christopher G. Bell and Stephan Beck; Email: christopher.bell@ucl.ac.uk and s.beck@ucl.ac.uk
Submitted: 07/18/12; Revised: 08/22/12; Accepted: 09/08/12
http://dx.doi.org/10.4161/epi.22127

The genetic loss and gain of CpG dinucleotides over evolutionary time will impact upon the epigenome. Genome-wide variation in GC content at the megabase scale led to the formation of isochores before mammalian radiation[24,25] with an increase in CpGs occurring ~90 million years ago (MYA).[26] A subsequent clock-like loss of CpGs, due to the time- not generation-dependent substitution rate of cytosine deamination,[27] has led to roughly similarly numbered, but differing sets of CpGs in primates. The mutability of individual CpGs can be determined by accounting for the influence of surrounding CpG density, as well as by sequence context and nucleosome position.[28,29] Regions of CpGs that remain hyperconserved have been found to co-locate with polycomb repressive complex 2 binding domains and developmental genes.[28]

On the other hand, GC increase is influenced by primate recombination rates.[30,31] So much so, that regions of extreme substitutional divergence in the human genome[32-34] co-locate with recombination-associated BGC.[35-39] This process therefore negates or obscures any potential evidence of weak selection.[39,40] BGC can lead to the formation of CGIs[11] and, furthermore, Cohen et al. have recently shown that CGIs can evolve without the requirement of selective pressure,[41] although a possible subtle influence on CpGs via gene body methylation may exist.[42]

Cytosine deamination is consequently the predominant single nucleotide mutational force, occurring at one order of magnitude higher in the genome than other single base substitutions. Conversely, a highly localized BGC-mediated increase of CpGs occurs, associated with recombination.[36,40] To discover the locations of potential species-specific regulatory modulation, due to CpG dinucleotide change, we identified a subset of human CpGs that were only present, either uniquely maintained or gained, in that lineage. While there are approximately ~40 million genetic differences between human and chimpanzee, the vast majority are due to random genetic drift.[43] Divergence at CpG sites between these two species is estimated to be at 15.2%, compared with 0.92% for other nucleotide substitutions.[43] Therefore, we used the additive collective power of multiple closely related species in a six-species inter-primate comparison.[44,45]

The CpG sequence can itself act as a genomic signaling molecule via combinatorial transcription factor binding specificity,[1,46] facilitate epigenomic variation by influencing CGI promoter amenable chromatin structure and gene body methylation.[47,48] Consequently we hypothesized that by identifying human-specific CpGs we may find potential regions of species-specific differential regulation.[5,42,49,50] The sequence comparative approach would be blind to any potential causative mechanisms. The novel CpG clusters identified may highlight genes where a species-specific shift in epigenetic control has been enabled by this genetic change. These regions would potentially be enriched for human traits, as well as the possibility of associations with disease susceptibilities that have arisen as a by-product of human evolution.

Results

Human-Specific CpGs. To uncover the subset of CpGs present only in the human lineage, an inter-primate comparison was performed by examining the Enredo-Pecan-Ortheus Whole-Genome Multiple Alignments Sequences for human, chimpanzee, gorilla, orang-utan, rhesus macaque and common marmoset (Ensembl Compara.6_primates_EPO).[51,52] This set of sequences contains 19,198 blocks and has been able to align 84.54% of the human genome. We parsed the blocks of this alignment requiring non-duplicated sequence in both human and chimpanzee and sequence of at least one other primate, which reduced our quasi-genomic set (referred to as h1c1o1: human, chimpanzee and other primate) to 79.99% of the human genome. This contained 25,100,205 or ~88.95% of the total haploid human CpGs. Each of these remaining CpGs was then interrogated with the requirement that at its precise position none of the other primates had a CpG dinucleotide present. Furthermore the chimpanzee sequence and the closest nearest other primate present in the alignment block (96.6% Gorilla) were required to have aligned sequence at this position i.e. was not N or -. This led to an initial human-specific subset of 1,820,319 CpGs. These CpGs were then conservatively filtered for polymorphism utilizing 1,000 genomes data removing any CpG with any evidence of variation, as a SNP, or within a copy number or structural variant,[53] leading to a final estimate of 1,192,484 human-specific CpGs.

CpG beacons. We define "beacons" as species-specific non-polymorphic DNA motifs able to carry both genetic and epigenetic information. According to the above analysis, we estimated the number of CpG beacons to be ~1.19 million in the human genome. In the future a definitive set will be able to be established following mass whole genome sequencing in a large number of these primates. However this current calculation will already be enriched for "true" human CpG beacons that can facilitate unique species-specific epigenomic variation. A user interface to view the human CpG beacons in the UCSC genome browser in the context of existing annotation is available at www2.cancer.ucl.ac.uk/medicalgenomics/humanCpGBeacons/trackList.php.

The density distribution of the human beacons in 1 kb windows was estimated, which showed more than half were singletons, ~2% were ≥ 5 beacons/kb, and 0.03% were ≥ 20 beacons/kb. To assess the significance of this long tail with higher density, we performed 1,000 permutations by choosing a set of random beacons from the CpG locations in the h1c1o1 genomic set. This simulation never exceeded the number of peaks that are ≥ 20 CpG beacons/kb in the observed genome set (peaks ≥ 20 CpG beacons/kb: simulation peaks range = 0–7, simulation average = 1.527 peak per genome, observed peaks = 21, empirical $p < 1 \times 10^{-3}$).

Extreme CpG beacon clusters. Taking this ≥ 20 CpG beacons/kb as an initial threshold (which reflects an increase of ≥ 4% in CpG density per kb in human compared with the other primates) we identified 21 extreme genomic outliers of human CpG beacon density (see **Table S1**). Beacon density distribution is displayed across the genome in **Figure 1**. This initial observation revealed that the third highest peak on Chromosome 20 colocated with the promoter CGI of the *HAR1A* gene, a non-coding gene significant in cortical development discovered by Pollard et al. (**Fig. S1**).[32] *HAR1A* was identified to be co-expressed by Cajal-Retzius neurons, with Reelin, a secreted glycoprotein that

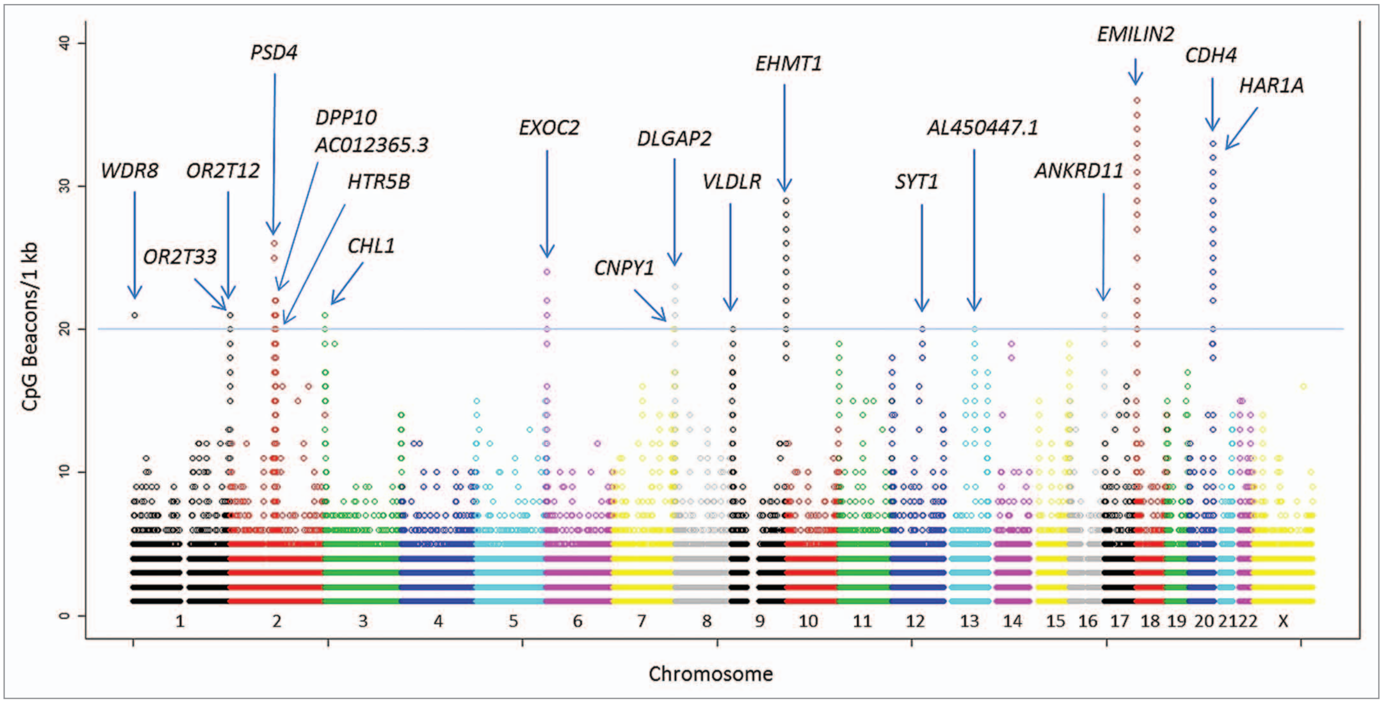

Figure 1. Human CpG beacons by 1 kb density score and genomic location. Loci greater than or equal to a threshold of 20/kb are indicated. A telomeric bias in peaks is evident, as well as in the historic chromosome 2q13 fusion point.[36]

is fundamental in specifying the six-layer structure of human cortex.[32] This gene had been first identified by mammalian and vertebrate comparative genomics for regions of high conservation but outlying substitution of any type in the human genome, with an extreme region of 118 bp containing 18 human changes since the Homo-Pan split. In fact eight of these substitutions are CpG beacon creating, from the total of 35 in this cluster that spans ~1.8 kb. This locus would still be a genomic CpG beacon cluster outlier with a peak of 24/kb even with this 118bp region removed. Therefore this critical non-coding gene was able to be identified without any recourse to longstanding vertebrate or mammalian conservation but purely by focusing on inter-primate CpG density change. Larger regions of bias identified across this locus have implicated recombination hotspot drift over time.[38,54]

We were therefore interested in the significance of the other 20 CpG beacon clusters identified in the human genome. We preformed gene set enrichment with Ingenuity Pathway Analysis (IPA, ©2011 Ingenuity Systems, Inc.) on these genes overlapping an extreme beacon cluster (70%), or within 100 kb 5' or 50 kb 3' of their transcript, and found highest significant enrichment for the categories of developmental and genetic disorder, inflammatory response, reproductive system development and function, and neurological disease genes [p value with Benjamini-Hochberg correction ($P_{\text{B-H}}$) = 6.03 × 10^{-3}, **Fig. S2**]. These 20 clusters included the causative genes when mutated for four different monogenic mental retardation disorders (*ANKRD11*,[55] *CHL1*,[56] *EHMT1*[57] and *VLDLR*[58,59]) and genes implicated in complex traits through GWAS and CNV analyses to phenotypes such as behavioral and psychiatric disorders including autism and bipolar disorder (*ANKRD11*,[60] *DLGAP2*[61] and *DPP10*[60,62]); synaptic transmission (*SYT1*[63]); as well as total cerebral brain volume in a radiological examination (*CDH4*[64]) (see **Table S1**). To take into consideration any possible gene size bias, we also performed an analysis using the regional based binomial test included in the GREAT gene enrichment analysis tool[65] (using default cut-offs but reducing the maximum distal extension from 1 Mb to 100 kb, see methods) for these 20 CpG beacon clusters, excluding the known *HAR1A* result. This was significant for only three categories of biological process with an FDR Q ≤ 0.15: which included the categories cognition (binomial raw p = 1.43 × 10^{-5}, FDR Q = 1.26 × 10^{-1}), and behavior (binomial raw p = 2.25 × 10^{-5}, FDR Q = 9.87 × 10^{-2}). Furthermore, as a negative control, we also calculated the locations of the Chimpanzee CpG beacon clusters that exceed the 20/kb threshold and these identified no genes implicated with developmental delay or mental retardation (see **Table S2**) and as well was non-significant with GREAT analysis (via liftOver to human).

The human CpG beacon clusters represent regions of potential regulatory modulation or change to the nearby genes that is human-specific. This correlation, and not causation within these regions, is of interest particularly as these monogenic disease genes have shown that genetic mutation within them is not lethal but carries significant developmental and neurological pathology. These important genes could therefore be the plausible targets of significant regulatory change between human and other closely related primates due to the similarity of their proteomes.[66]

Biased-gene conversion overlap. The human extreme beacon clusters showed very strong overlap with the top 200 regions of BGC identified by Drezser et al. (57.1% of ≥ 20 CpG beacons/kb clusters, χ^2 p < 2.20 × 10^{-16}),[36] thus implicating localized GC

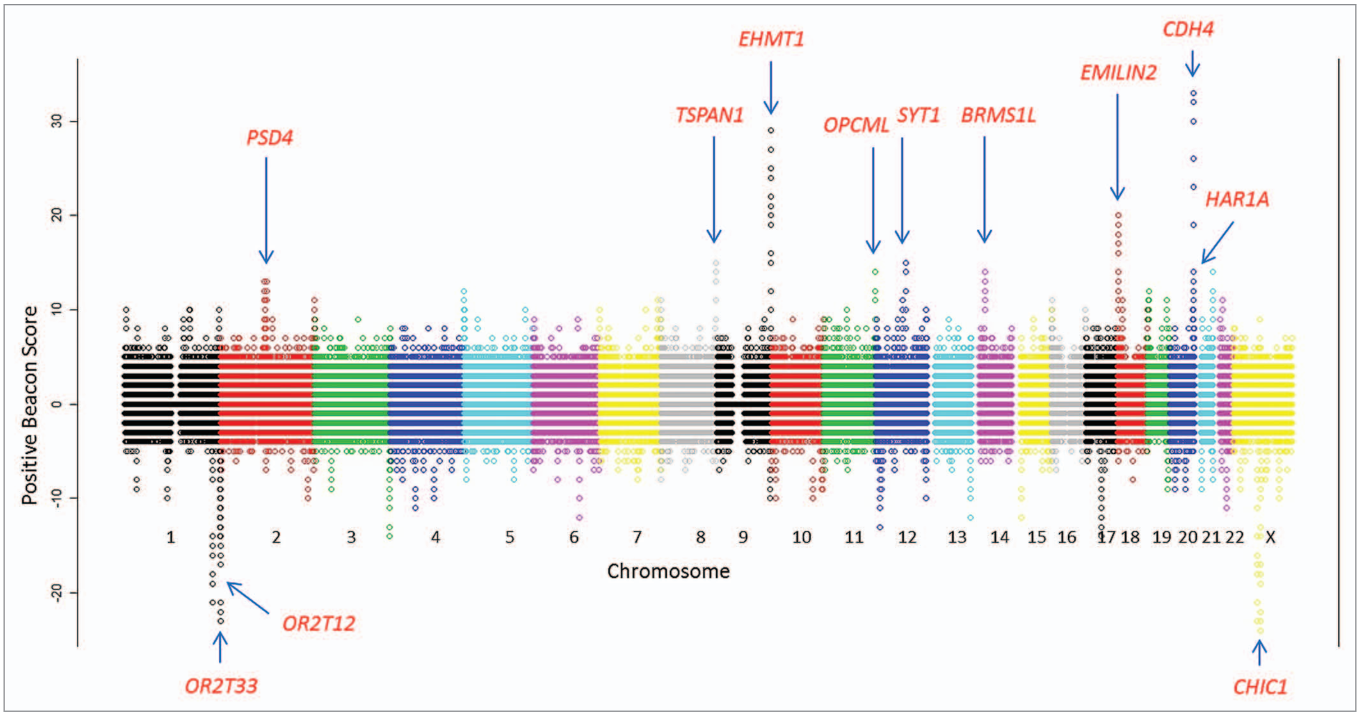

Figure 2. Human positive CpG beacon scores calculated across the genome in 1 kb windows with 100 bp slide. Extreme positive or negative loci are indicated.

rise, which is thought to be a neutral process, with a consequent increase in CpGs. Therefore this implies the CpG beacon clusters associate with a recombination driven CpG increase in human, as opposed to regions of high CpG mutability in other primates. Moreover, we also identified the majority of these clusters in telomeric regions (52.3% in terminal chromosome bands), which are known to have elevated rates of recombination in males,[67] with hotspots associated with BGC.[40] A 15% greater divergence in terminal ends of chromosomes was identified in the chimpanzee sequencing project.[8]

Cohen et al. recently reclassified CGIs using evolutionary modeling into those that were classical hypo deaminated islands, with ~80% of these 10 kb from a transcription start site (TSS) and with strong overlap with H3K4me3, and those that had arisen as a by-product of BGC that were typically constitutively hypermethylated.[41] However, on examination of the available sperm methylome data via MeDIP-seq,[68] which includes data for 18 of these extreme beacon cluster regions that co-located with CGI, these were found to be predominately hypomethylated. The average methylation level was 26.38%, therefore aiding the retention of CpGs by reduced mutability, enabling potential regulation by methylation to occur.[10]

Positive CpG beacon clusters. To differentiate between specific CpG increase, as opposed to generalized regions of GC rise, we controlled by the concurrent formation of the exact inverse dinucleotide GpC; which lacks methylation ability. We defined Positive CpG Beacon Clusters (PBCs) as regions where CpG beacons outweighed their local human-specific GpC content. BGC increases regional GC content and therefore passively CpGs, but if CpGs are methylated in the germ line their continual loss will eventually lead to the acquired GpCs outweighing CpGs over time. We calculated this via a sliding window analysis with a window size of 1 kb and slide of 100 bp across the genome (see **Fig. 2**). The vast majority of the extreme beacon clusters were genomic outliers of PBC score, *i.e. EHMT1* and *CDH4* and all except two possessed positive scores (see **Table S1**). These two extreme negative scores were identified in loci known for extensive and continual gene conversion, the olfactory receptors, with PBC score peaks of -23/kb and -16/kb for *OR2T3* and *OR2T12,* respectively.

Extreme CpG beacon clusters appear to be strongly driven by BGC; therefore, PBCs indicate regions where the gained CpGs beacons are not as hypermutable as would be expected, likely due to a loss of methylation in germ line. By retaining from the 20 clusters only those with at least a +5 PBC score, more significant p values in both biological category enrichments of cognition and behavior were obtained (binomial $p = 7.19 \times 10^{-6}$ and 9.41×10^{-6}, Q FDR value = 6.3×10^{-2} and 4.1×10^{-2}, respectively). To explore the potential of this CpG beacon-specific increase genome-wide, we identified all the PBC ≥ +5 loci comprising 2,601 regions, that account for ~0.1% of the human genome. IPA analysis of associated PBC genes showed significant results for a large number of common disease categories ($P_{\text{B-H}} < 1 \times 10^{-20}$) (data not shown), although this result will be biased disproportionally with larger gene regions. Examining these PBC loci with GREAT (genomic regions enrichment of annotation tool) analysis, which corrects for this issue of potential genomic space available to input signal, we identified a number of significant results for potential human phenotypes and traits (see **Table S3**, FDR Q < 0.05), such as cortical gyral simplification (binomial FDR Q-value = 1.94

$\times 10^{-4}$), atrophy/degeneration affecting the central nervous system ($Q = 1.69 \times 10^{-2}$), abnormality of the cerebral cortex ($Q = 2.23 \times 10^{-2}$) and poor speech ($Q = 4.66 \times 10^{-2}$). A large number of biological processes were implicated as significant, including the nucleus accumbens development ($Q = 6.31 \times 10^{-7}$), nose development ($Q = 4.52 \times 10^{-6}$) and neurotransmitter transport ($Q = 1.27 \times 10^{-2}$) (see **Table S4**).

These PBCs regions were also enriched in intragenic islands (CGI within transcripts but not at the classical 5' promoter region), being found twice as commonly within these regions as would be expected for their genomic size (see **Fig. S3**, χ^2 $p < 2.20 \times 10^{-16}$). In fact, with increasing CpG beacon density this intragenic enrichment became stronger (see **Fig. S4**, Beacons ≥ 10, χ^2 $p < 2.20 \times 10^{-16}$). These islands have been implicated in a number of other studies for their significant role in developmentally important isoforms.[5,69,70] Examination of repeat classes identified enrichment in the hominid-specific SVA subclass[71,72] (see **Fig. S5**, χ^2 $p < 2.20 \times 10^{-16}$), which arose ~20 MYA and has been extremely prolific during evolution of the primate genome.[73,74]

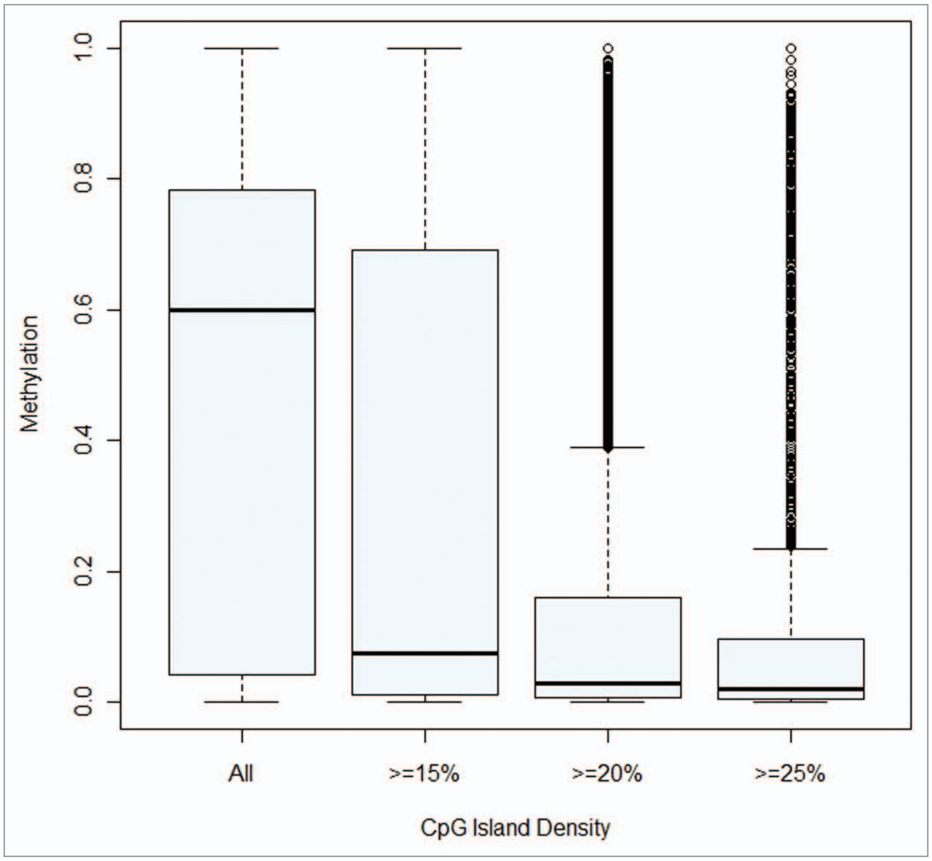

Figure 3. CpG density influence on methylation in Wu et al. CpG Islands from Li et al. bisulphite methylome data from peripheral blood mononuclear cell DNA (Kruskal-Wallis rank sum test p value $< 2.2 \times 10^{-16}$).[77,78]

Correlation between CpG density and CGI hypomethylation. While specific genetic methylation-determining regions (MDRs[75]) have been identified within CGIs, a correlation with CpG density and hypomethylation has also previously been recognized.[10] Therefore, CpG beacon clusters will lead to species-specific CpG density increases which may be associated with increased CGI hypomethylation and formation of permissive chromatin.[76] A CpG density of ~20% CpGs (or 10% methylatable cytosines) was proposed by Eckhardt et al.[19] as a threshold beyond which CGI are highly likely to be constitutively unmethylated across all differentiated tissues. Examining the available data from two bisulphite sequencing experiments from Li et al.[77] in peripheral blood cells and Lister et al.[2] from fibroblasts, we find methylation within CGIs is strongly correlated in these sets ($r^2 = 0.84$), despite being confounded by different experiments, tissues and cell line effects. Furthermore, the same significant trend of reduced methylation when CGIs were categorized into subgroups of all, ≥ 15%, ≥ 20%, ≥ 25% CpG density is seen using both the Ensembl CGI definition and an alternate CGI set by Wu et al. identified via hidden Markov models.[78] (Kruskal-Wallis $p < 2.2 \times 10^{-16}$) (**Fig. 3**; **Fig. S6A–C**).

Next, we generated peripheral blood cell methylome data by MeDIP-seq of pooled samples from chimpanzee and rhesus macaque as well as pooled human samples. Examination of these data also supported the inverse correlation of CpG density with methylation in CGI across all three species in the Ensembl CGI set (see **Fig. S7A**, $p < 2.2 \times 10^{-16}$) and as well the Wu et al. CGIs that are proposed to have improved trans-species CGI prediction (**Fig. S7B**, $p < 2.2 \times 10^{-16}$).[78]

We then investigated whether the influence on methylation change was still apparent in CpG density that changed over time in orthologous CGI between these species. We identified the orthologous CGI set between human and chimpanzee (Ensembl n = 13,999, Wu et al. n = 34,053), and human and macaque (Ensembl n = 4,654, Wu et al. n = 19,200) and chimpanzee and macaque (Ensembl n = 4,004, Wu et al. n = 18,747). For example, the orthologous *DPP10* CpG beacons extreme cluster CGI, showed average methylation (RPM) of 0.51 and 4.80 in human and chimpanzee respectively, but not enough CpG density in macaque for a CGI to be defined even by the Wu et al. methodology. The subset of these orthologous islands that were ≥ 20% CpG density in one species and ≤ 19% in the other was then obtained. A significant difference was identified in the Ensembl set for human vs. chimpanzee CGI (Wilcoxon $p = 1.954 \times 10^{-12}$; data not shown) and in the larger Wu et al. set these groupings showed a small but significant reduction in methylation [expressed as average reads per million (RPM)] consistently in the higher density CGI group across all species comparisons (see **Fig. 4**, all p Wilcoxon $< 2.2 \times 10^{-16}$).

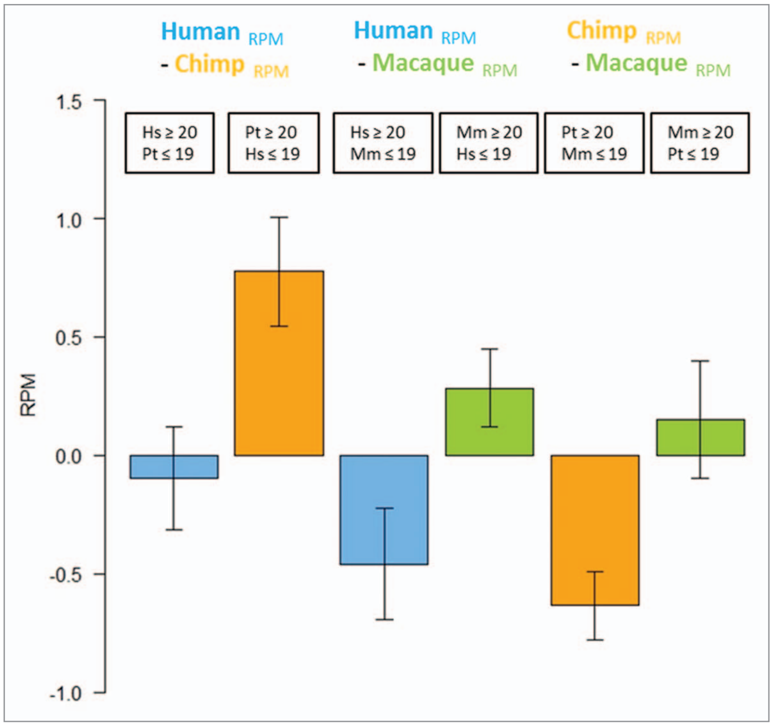

Figure 4. Comparison of methylation in subset of orthologous CGI set from Wu et al.[78] The RPM in these islands was compared by subtraction. First Human[RPM] – Chimpanzee[RPM], in islands Human (Hs) > 20% CpG and Chimpanzee (Pt) < 19% CpG then Chimpanzee > 20% CpG and Human < 19% CpG. Then Human[RPM] – Macaque[RPM], Human (Hs) > 20% CpG and Macaque (Mm) < 19% CpG and Macaque > 20% CpG and Human < 19% CpG. Finally Chimpanzee [RPM] – Macaque [RPM] in islands Chimpanzee > 20% CpG and Macaque < 19% CpG then Macaque > 20% CpG and Chimpanzee < 19% CpG. All show a consistent pattern where the less CpG dense island (< 19%) is more methylated than the more CpG dense island (> 20%).

Therefore, we have shown that varying CpG density changes the methylation potential within CGIs. This change in likelihood of methylation between low and high density CGIs was found to occur across and between the three species. The most extreme human-specific genomic eruptions of CpGs occur in the identified "CpG beacon" clusters, which in turn have highlighted genes associated with human traits and disease.

Discussion

The proteome is similar across placental mammals; therefore, the creation of new protein coding genes is rare,[79] although not unknown.[80] Regulatory modification has long been proposed as critical in human acquired traits[66] and genomic data acquired in the last decade supports the hypothesis that species evolution is predominately via novel regulatory adaptation and subsequent altered gene expression.[79,81] Recently, the identification of human-specific loss of regulatory DNA revealed insights into human evolutionary divergence.[82]

Epigenetic mechanisms, including DNA methylation, are critical in genome regulation and viable mammalian development requires the ability to methylate cytosines.[83] This chemical modification can lead to disparate effects depending on genomic location; repressive in CGI,[18] activating in gene bodies[47] and splicing influence in CTCF binding sites.[84] Changes in developmental timing are significant in species-specific differences[85] and the epigenetic modulation of intragenic islands may direct developmentally critical isoforms.[5,86] Thus, this epigenomic extra layer of control enables additional axes to the adaptive landscape and aids in the evolution of complex phenotypes.[23,87] Cytosine methylation has also been suggested to be significant in karyotype evolution.[88] Even simply focusing on human higher cognitive functioning, notwithstanding all the other phenotypic differences, levels of brain tissue-specific imprinting,[89,90] distinctive neuronal DNA methylation profiles[91,92] and potential role in synaptic plasticity,[93] as well as pathogenic Methyl Binding Domain gene mutations in post-natal brain development disorders,[94,95] all postulate that the gain and loss of CpG may be fundamental in the human-specific phenotype.

We therefore identified a subset of species-specific CpGs by inter-primate comparison, impartial to mechanistic cause, which we have termed CpG beacons. Focusing initially on extreme human CpG beacon clusters, we showed they are enriched for neurological disease genes and, additionally, co-locate with the evolutionary accelerated *HAR1A* nc-RNA gene. A strong correlation between accelerated genomic loci and bias toward increased GC content was observed previously,[35] due to the effects of recombination.[30] Fine scale recombination hotspots show high diversity between human and chimpanzee, as they are short-lived relative to divergence times,[96,97] potentially strongly influenced by the variation in zinc finger binding of *PRDM9*.[98,99] GC-coupled CpG increase due to recombination has been suggested to have played a considerable role in CGI formation[11] and thus may be a strong driver in the formation of CpG beacon clusters and thus species-specific regulation.

However, on top of the localized strong effect of BGC on increased GC, multiple subtle substitutions have been shown to have a morphological evolution effect altering the timing and level of expression.[100] We looked for potential CpG-specific signatures by identifying where human-specific CpG exceeded human-specific GpC, defining Positive CpG Beacon Clusters, which identified potential human traits that may have arisen during human evolution.[101]

Recent comparative methylome analyses have revealed species-specific differences.[102,103] Molaro et al. examined chimpanzee and human sperm and supported the link between genome and epigenome, by identifying strong CpG decay correlated with methylation over brief evolutionary periods. They also found extensive species-specific methylation differences in SVA repeats, with significantly increased numbers of orthologous hypomethylated SVAs within humans. Interestingly, this is the same subtype in which we identified high enrichment of positive beacon clusters, which could be driving this hypomethylation. Additionally SVAs

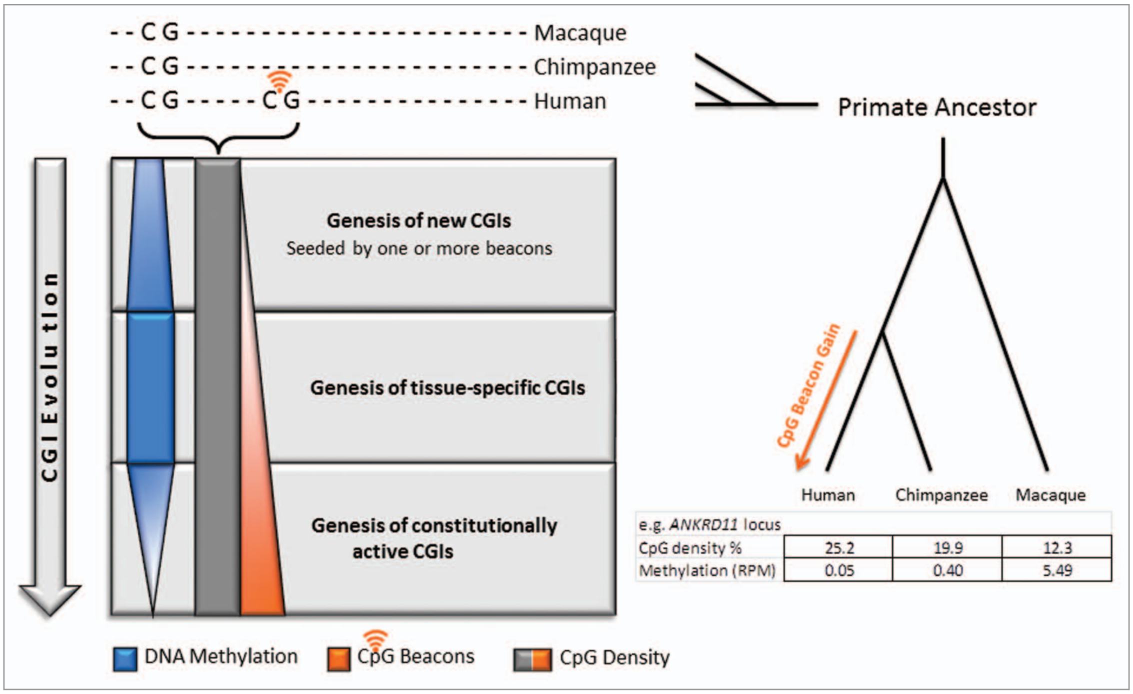
- - C G - Macaque
- - C G - Chimpanzee
- - C G - - - - - C G - - - - - - - - - - - - - - - Human
Primate Ancestor
C G I Evolution
Genesis of new CGIs
Seeded by one or more beacons
Genesis of tissue-specific CGIs
Genesis of constitutionally active CGIs
CpG Beacon Gain
Human
Chimpanzee
Macaque
DNA Methylation
CpG Beacons
CpG Density

e.g. *ANKRD11* locus			
CpG density %	25.2	19.9	12.3
Methylation (RPM)	0.05	0.40	5.49

Figure 5. Model for beacon-mediated CGI evolution and example for possible association with disease. The left panel illustrates a model for CpG beacon-mediated increase of CpG density. A moderate CpG beacon increase lead to the formation of low density CGIs which are predominantly methylated and prone to tissue-specific methylation. Further CpG beacon increase can eventually lead to high density CGIs with increased likelihood of becoming constitutively hypomethylated. Variation in such CGIs could then result in species-specific phenotypic changes as discussed in this study for CGIs containing extreme clusters of > 20 beacons per kb. CpG beacon gain may indicate reduced mutability due to acquisition of new methylation determining regions,[75] direct gain due to accumulated substitution or biased gene conversion, or a combination of all of these processes. The right panel shows an example of one of the identified extreme CpG beacon cluster containing CGIs that is associated with the human *ANKRD11* gene, implicated in Autism. In this case, the CpG density and methylation state of the orthologous CGIs in human, chimpanzee and macaque are concordant with the proposed model. Methylation values were determined by MeDIP-seq and are given as reads per million (RPM).

have recently been identified to be involved in active somatic retrotransposiotn in human brain.[104]

Lienart et al. have recently identified the existence of methylation-determining regions (MDRs) due to sequence characteristics within CGI, but also acknowledged the necessity of a critical CpG density within these regions.[75] Increasing CpG density forms low density CpG islands which are more likely to have variable methylation and hence to be tissue-specific or developmental time-dependent. Further density rise will create high density islands that eventually will become increasingly likely to become constitutively hypomethylated above a threshold identified earlier by Eckhardt et al.[19] This correlation can be seen by re-examination of the Li et al.[77] and Lister et al.[2] bisulphite sequencing data and is supported across three species in this study via MeDIP-seq. Either MDR-induced CpG retention, BGC created CpGs, or potentially both can lead to clusters of CpGs resulting in hypomethylated islands that then recruit factors such as Cfp1. While this process does not lead to explicit expression per se, it establishes open permissive chromatin via H3K4me3 marked domains.[12,76] Therefore, CpG beacons have the capacity to move, or indicate the movement of, these loci along a continuum from no island to tissue-specific island to constitutively active island, as illustrated in the model shown in **Figure 5**.

In conclusion, the CpG dinucleotide is vital for regulation and not only transmits genomic data but also enables epigenomic variation. Thus, genomic change in this dynamic dinucleotide required for DNA methylation, influencing CGI methylation, gene body methylation, imprinting and splicing, is fundamental to understanding our evolutionary acquired traits and vulnerabilities to disease.

Methods

CpG beacon identification. CpG loss is time- not replication-dependent; therefore, there are almost equal counts of CpG in human and chimpanzee.[43] Recent estimates from whole genome sequencing for mutation rate is ~1 × 10^{-8} per generation[105] with the CpG dinucleotide approximately ten times this. Due to the rapid turnover in regulatory elements,[106] most are too weakly conserved to mouse to distinguish[45] which will particularly be the case with the highly mutable CpGs. By utilizing the additive collective divergence of multiple primates[44,45] a CpG's human-specific state was attributed. The comparatively inferior sequence quality of these individual non-human primate sequences was balanced by the combined multispecies comparison vs. human. Assignment of ancestral state by use of chimpanzee alone was found to have an error rate of 0.65% utilizing macaque as a second out-group.[107] Furthermore, most SNPs have been calculated to be < 1 million years of age, compared with the minimum divergence time of chimpanzee and human which is estimated at 5 million years.[108]

Therefore, to identify the human-specific changes we utilized the Ensembl Compara.6_primates_EPO six primates alignment[51,52] build 58. This includes the species *Homo sapiens*, *Pan troglodytes*, *Gorilla gorilla*, *Pongo abelii*, *Macaca mulatta* and *Callithrix jacchus*. The builds included are human GRCh37, chimpanzee Mar. 2006 (CGSC 2.1/pan Trog2), gorilla (gorGor3); orang-utan Jul 2007 (WUSTL version Pongo_albelii-2.0.2); macaque Jan 2006 (MGSC Merged 1.0/rheMac2); and marmoset Mar 2009 (WUGSC 3.2 (GCA_000004665.1)). The Ensembl Compara.6_primates_EPO alignment blocks was then reduced in a stepwise fashion due to the requirement of: unique human sequence, i.e. does not align to greater than one location in human genome (82.71% of human genome remaining); unique chimpanzee sequence (80.54%); and contains at least one other primate (79.99%) in order to utilize the strength of the inter-primate comparison.[45] Within this ~80% of the human genome that was able to be aligned, an algorithm was devised to identify the location of each human CpG site within these blocks and then compared with the corresponding bases in other species. To be identified as a potential human-specific CpG, the requirement in chimpanzee sequence was that it did not match CG and did not contain N or –. All other species sequences at this position also did not match CpG and the closest other primate (gorilla in 96.64% of sites) did not contain N or –. If this was the case then it was recorded as a human-specific CpG site, which led to a set of 1,820,319 CpGs. All human cluster locations are given in build Human GRCh37 coordinates. The chimpanzee beacons were calculated using the exact same methodological algorithm as the human, but instead changing the focused species to *Pan troglodytes*.

Polymorphic filter. Any CpG with evidence of polymorphism from 1,000 Genomes data for SNP, CNV and Indel was then removed from the set. The December 2010 Data update Full Project Genotype Release from calls on 629 individuals from the 20100804 sequence was used. Indel data was from the February 2011 update, which were calls from Dindel on the same 629 individuals from the 20100804 sequence and alignment, and also available CNV data from 179 unrelated individuals.[109] This resulted in a non-polymorphic human set of 1,192,484 CpGs.

CpG beacon density calculation and permutations. Initial density permutations were calculated for each CpG beacon by counting the number of CpG beacons within a region of 499 bp downstream and 500 bp upstream. Random beacon sets of the same number 1,192,484 were generated from the total set of locations of CpGs in the h1c1o1 genome set of 20,207,732 and density calculated.

Positive CpG beacon clusters. Positive beacon clusters were calculated, via a sliding window of 1 kb and slide of 100 bases across the genome. The total non-polymorphic human-specific GpCs within the 1kb region was subtracted from the total CpG beacons within this region.

$$\text{Positive CpG Beacon Score} = \frac{(\text{CpG beacons} - \text{human specific GpCs})}{1\ kb}$$

Gene set enrichment analyses. Ingenuity Pathway Analysis ©IPA was performed for gene set enrichment. The location of clusters was assigned to genes if it mapped to within 100k 5' and 50k 3' of the transcript. The following IPA analysis settings were used: Reference set: Ingenuity Knowledge Base (Genes Only), Relationship to include: Direct and Indirect, Includes Endogenous Chemicals. Optional Analyses: My Pathways My List. Filter Summary: Consider only molecules and/or relationships where (species = Human) AND (confidence = Experimentally Observed). Benjamini-Hochberg multiple test corrected p values are shown only. The region-based binomial analysis of GREAT analysis 2.0.1[65] was utilized to identify genome regional enrichments from the location of the extreme beacon clusters, as well as the moderate positive beacons clusters ≥ 5. This takes into consideration the bias of potential genomic space available compared with the traditional hypergeometric test. The parameters used were association by Basal plus extension with default values of proximal 5 kb upstream, 1 kb downstream, but a reduced distal limit to 100 kb from 1 Mb and significance assessed by the regional based Binomial test FDR Q value.

Publicly available bisulphite sequencing data. The Lister et al. fibroblast methylome data was downloaded from http://neomorph.salk.edu/human_methylome/data.html. The Li et al. PBMC methylome data was downloaded from the NCBI Gene Expression Omnibus (www.ncbi.nlm.nih.gov/geo/query/acc.cgi?acc = GSE17972). For the Lister et al. and Li et al. data sets individual CpG methylation was calculated by combining the reads from the two strands and subsequently requiring a five read minimum coverage for inclusion.

Comparative MeDIP-seq. DNA was extracted from peripheral blood of five chimpanzees (*Pan troglodytes*, three males, two females) and five rhesus macaques (*Macaca mulatta*, three males, two females). Samples were taken from captive individuals at Tierpark Nordhorn, Basel Zoo, Leipzig Zoo and at the German Primate Center during routine health checks and not specifically for this study. Microsatellite analysis conducted at the German Primate Center verified that respective individuals are not related. Sample collection adhered to the American Society of Primatologists (ASP) Principles for the Ethical Treatment of Non-Human Primates (www.asp.org/society/resolutions/EthicalTreatmentOfNonHumanPrimates.cfm).

To obtain averaged methylomes and reduce individual genotype effects, DNAs were pooled for each species at equal concentration for each individual. MeDIP was then executed according to Auto-MeDIP-seq protocol as described previously[110] and sequenced on Illumina GAIIx. This was performed with paired end reads of 36 bp with average fragment sizes of: 197 bp in human, 222 bp in chimpanzee, and 217 bp in macaque. The corresponding methylome data are available from the authors on request. A comprehensive analysis of these methylomes will be described elsewhere (Wilson G.A. et al., manuscript in preparation).

MeDIP-seq data was processed using MeDUSA (methylated DNA utility for sequence analysis).[111] This computational pipeline performs a full analysis of MeDIP-seq data by utilizing a number of freely available software packages. Raw sequence data in fastq format were aligned to the reference genomes (Human GRCh37, panTro2 and rheMac2) using alignment software BWA (v0.5.8),[112] with default parameters, to generate a SAM format alignment file. Aligned reads were filtered using SAMtools (v0.1.9)[113] to remove reads that failed to form a correctly aligned pair (forward and reverse templates). Further filtering based on mapping score was also performed (read pair must contain read with mapping quality ≥ 10). Potential PCR artifacts were removed by discarding all but one read within groups of non-unique reads (i.e., reads aligned to the exact same start and stop position on the same chromosome). FastQC (www.bioinformatics.bbsrc.ac.uk/projects/fastqc) was used to determine sequence data was of acceptable quality and the Bioconductor (v2.7)[114] package MEDIPS (v1.0.0)[115] performed enrichment and coverage analyses. Reads per million (RPM) was calculated within regions as (reads/total reads) times 10^6 for each species (total human reads = 40,797,356, chimpanzee = 32,910,189 and macaque = 24,933,164).

Genetic influence on the DNA methylome. The MEDIPS package was used to approximate absolute methylation scores from relative MeDIP results.[115] This enables regional methylation to be compared over features, i.e., CpG Islands utilizing the appropriate genome sequence for each species. LiftOver[116] was used to calculate orthologous CGI sets with overlap of at least 95% required. Greater than 20% and less than 19% orthologous sets were chosen from the orthologous island sets for each grouping with the following numbers: Hs ≥ 20 and Pt ≤ 19, Ensembl = 375, Wu = 557; Pt ≥ 20 and Hs ≤ 19, Ensembl = 150, Wu = 614; Hs ≥ 20 and Mm ≤ 19, Ensembl = 248, Wu = 605; Mm ≥ 20 and Hs ≤ 19 Ensembl = 62, Wu = 1530; Pt ≥ 20 and Mm ≤ 19, Ensembl = 256, Wu = 700; Mm ≥ 20 and Pt ≤ 19 Ensembl = 118, Wu = 1451 (Hs, *Homo sapiens*; Pt, *Pan troglodytes;* Mm, *Macaca mulata*).

Statistical analysis. Statistical calculations were performed in the R statistical environment.[117] Empirical p values were calculated as the excess of simulation vs. observed values. Kruskal-Wallis rank sum test was used to compare methylation in CGI density sets and Wilcoxon test for comparison between average RPM values for orthologous island sets. Chi-square calculations for enrichments were performed for PBC by bases covered of PBC vs. total bases of category and CpG beacon vs. total CpGs.

Disclosure of Potential Conflicts of Interest

No potential conflicts of interest were disclosed.

Acknowledgments

We thank the staff of the Tierpark Nordhorn, Basel Zoo, Leipzig Zoo and the German Primate Center for providing blood samples of chimpanzees and rhesus macaques. Work in the Beck lab was supported by the Wellcome Trust (084071), Royal Society Wolfson Research Merit Award (WM100023) and EU-FP7 projects HEROIC (018883), EPIGENESYS (257082) and BLUEPRINT (282510).

Author Contributions

Conceived and designed the experiments: C.G.B., G.A.W. and S.B. Performed the experiments: C.G.B., L.M.B. and G.A.W. Analyzed the data: C.G.B. and G.A.W. Contributed reagents/materials/analysis tools: C.R. and L.W. Wrote the paper: C.G.B. and S.B.

Supplemental Materials

Supplemental materials may be found here:
www.landesbioscience.com/journals/epigenetics/article/22127

References

1. Bird A. The dinucleotide CG as a genomic signalling module. J Mol Biol 2011; 409:47-53; PMID:21295585; http://dx.doi.org/10.1016/j.jmb.2011.01.056.
2. Lister R, Pelizzola M, Dowen RH, Hawkins RD, Hon G, Tonti-Filippini J, et al. Human DNA methylomes at base resolution show widespread epigenomic differences. Nature 2009; 462:315-22; PMID:19829295; http://dx.doi.org/10.1038/nature08514.
3. Jones PA, Takai D. The role of DNA methylation in mammalian epigenetics. Science 2001; 293:1068-70; PMID:11498573; http://dx.doi.org/10.1126/science.1063852.
4. Jaenisch R, Bird A. Epigenetic regulation of gene expression: how the genome integrates intrinsic and environmental signals. Nat Genet 2003; 33(Suppl):245-54; PMID:12610534; http://dx.doi.org/10.1038/ng1089.
5. Maunakea AK, Nagarajan RP, Bilenky M, Ballinger TJ, D'Souza C, Fouse SD, et al. Conserved role of intragenic DNA methylation in regulating alternative promoters. Nature 2010; 466:253-7; PMID:20613842; http://dx.doi.org/10.1038/nature09165.
6. Ji H, Ehrlich LI, Seita J, Murakami P, Doi A, Lindau P, et al. Comprehensive methylome map of lineage commitment from haematopoietic progenitors. Nature 2010; 467:338-42; PMID:20720541; http://dx.doi.org/10.1038/nature09367.
7. Duncan BK, Miller JH. Mutagenic deamination of cytosine residues in DNA. Nature 1980; 287:560-1; PMID:6999365; http://dx.doi.org/10.1038/287560a0.
8. Chimpanzee Sequencing and Analysis Consortium. Initial sequence of the chimpanzee genome and comparison with the human genome. Nature 2005; 437:69-87; PMID:16136131; http://dx.doi.org/10.1038/nature04072.
9. Roach JC, Glusman G, Smit AF, Huff CD, Hubley R, Shannon PT, et al. Analysis of genetic inheritance in a family quartet by whole-genome sequencing. Science 2010; 328:636-9; PMID:20220176; http://dx.doi.org/10.1126/science.1186802.
10. Weber M, Hellmann I, Stadler MB, Ramos L, Pääbo S, Rebhan M, et al. Distribution, silencing potential and evolutionary impact of promoter DNA methylation in the human genome. Nat Genet 2007; 39:457-66; PMID:17334365; http://dx.doi.org/10.1038/ng1990.
11. Polak P, Arndt PF. Long-range bidirectional strand asymmetries originate at CpG islands in the human genome. Genome Biol Evol 2009; 1:189-97; PMID:20333189; http://dx.doi.org/10.1093/gbe/evp024.
12. Thomson JP, Skene PJ, Selfridge J, Clouaire T, Guy J, Webb S, et al. CpG islands influence chromatin structure via the CpG-binding protein Cfp1. Nature 2010; 464:1082-6; PMID:20393567; http://dx.doi.org/10.1038/nature08924.
13. Blackledge NP, Zhou JC, Tolstorukov MY, Farcas AM, Park PJ, Klose RJ. CpG islands recruit a histone H3 lysine 36 demethylase. Mol Cell 2010; 38:179-90; PMID:20417597; http://dx.doi.org/10.1016/j.molcel.2010.04.009.
14. Straussman R, Nejman D, Roberts D, Steinfeld I, Blum B, Benvenisty N, et al. Developmental programming of CpG island methylation profiles in the human genome. Nat Struct Mol Biol 2009; 16:564-71; PMID:19377480; http://dx.doi.org/10.1038/nsmb.1594.
15. Saxonov S, Berg P, Brutlag DL. A genome-wide analysis of CpG dinucleotides in the human genome distinguishes two distinct classes of promoters. Proc Natl Acad Sci U S A 2006; 103:1412-7; PMID:16432200; http://dx.doi.org/10.1073/pnas.0510310103.
16. Illingworth RS, Bird AP. CpG islands--'a rough guide'. FEBS Lett 2009; 583:1713-20; PMID:19376112; http://dx.doi.org/10.1016/j.febslet.2009.04.012.
17. Guenther MG, Levine SS, Boyer LA, Jaenisch R, Young RA. A chromatin landmark and transcription initiation at most promoters in human cells. Cell 2007; 130:77-88; PMID:17632057; http://dx.doi.org/10.1016/j.cell.2007.05.042.
18. Bird A. DNA methylation patterns and epigenetic memory. Genes Dev 2002; 16:6-21; PMID:11782440; http://dx.doi.org/10.1101/gad.947102.

19. Eckhardt F, Lewin J, Cortese R, Rakyan VK, Attwood J, Burger M, et al. DNA methylation profiling of human chromosomes 6, 20 and 22. Nat Genet 2006; 38:1378-85; PMID:17072317; http://dx.doi.org/10.1038/ng1909.

20. Irizarry RA, Ladd-Acosta C, Wen B, Wu Z, Montano C, Onyango P, et al. The human colon cancer methylome shows similar hypo- and hypermethylation at conserved tissue-specific CpG island shores. Nat Genet 2009; 41:178-86; PMID:19151715; http://dx.doi.org/10.1038/ng.298.

21. Doi A, Park IH, Wen B, Murakami P, Aryee MJ, Irizarry R, et al. Differential methylation of tissue- and cancer-specific CpG island shores distinguishes human induced pluripotent stem cells, embryonic stem cells and fibroblasts. Nat Genet 2009; 41:1350-3; PMID:19881528; http://dx.doi.org/10.1038/ng.471.

22. Hansen KD, Timp W, Bravo HC, Sabunciyan S, Langmead B, McDonald OG, et al. Increased methylation variation in epigenetic domains across cancer types. Nat Genet 2011; 43:768-75; PMID:21706001; http://dx.doi.org/10.1038/ng.865.

23. Feinberg AP, Irizarry RA. Evolution in health and medicine Sackler colloquium: Stochastic epigenetic variation as a driving force of development, evolutionary adaptation, and disease. Proc Natl Acad Sci U S A 2010; 107(Suppl 1):1757-64; PMID:20080672; http://dx.doi.org/10.1073/pnas.0906183107.

24. Nekrutenko A, Li WH. Assessment of compositional heterogeneity within and between eukaryotic genomes. Genome Res 2000; 10:1986-95; PMID:11116093; http://dx.doi.org/10.1101/gr.10.12.1986.

25. Eyre-Walker A, Hurst LD. The evolution of isochores. Nat Rev Genet 2001; 2:549-55; PMID:11433361; http://dx.doi.org/10.1038/35080577.

26. Arndt PF, Petrov DA, Hwa T. Distinct changes of genomic biases in nucleotide substitution at the time of Mammalian radiation. Mol Biol Evol 2003; 20:1887-96; PMID:12885958; http://dx.doi.org/10.1093/molbev/msg204.

27. Hwang DG, Green P. Bayesian Markov chain Monte Carlo sequence analysis reveals varying neutral substitution patterns in mammalian evolution. Proc Natl Acad Sci U S A 2004; 101:13994-4001; PMID:15292512; http://dx.doi.org/10.1073/pnas.0404142101.

28. Tanay A, O'Donnell AH, Damelin M, Bestor TH. Hyperconserved CpG domains underlie Polycomb-binding sites. Proc Natl Acad Sci U S A 2007; 104:5521-6; PMID:17376869; http://dx.doi.org/10.1073/pnas.0609746104.

29. Tolstorukov MY, Volfovsky N, Stephens RM, Park PJ. Impact of chromatin structure on sequence variability in the human genome. Nat Struct Mol Biol 2011; 18:510-5; PMID:21399641; http://dx.doi.org/10.1038/nsmb.2012.

30. Meunier J, Duret L. Recombination drives the evolution of GC-content in the human genome. Mol Biol Evol 2004; 21:984-90; PMID:14963104; http://dx.doi.org/10.1093/molbev/msh070.

31. Romiguier J, Ranwez V, Douzery EJ, Galtier N. Contrasting GC-content dynamics across 33 mammalian genomes: relationship with life-history traits and chromosome sizes. Genome Res 2010; 20:1001-9; PMID:20530252; http://dx.doi.org/10.1101/gr.104372.109.

32. Pollard KS, Salama SR, Lambert N, Lambot MA, Coppens S, Pedersen JS, et al. An RNA gene expressed during cortical development evolved rapidly in humans. Nature 2006; 443:167-72; PMID:16915236; http://dx.doi.org/10.1038/nature05113.

33. Prabhakar S, Noonan JP, Pääbo S, Rubin EM. Accelerated evolution of conserved noncoding sequences in humans. Science 2006; 314:786; PMID:17082449; http://dx.doi.org/10.1126/science.1130738.

34. Bird CP, Stranger BE, Liu M, Thomas DJ, Ingle CE, Beazley C, et al. Fast-evolving noncoding sequences in the human genome. Genome Biol 2007; 8:R118; PMID:17578567; http://dx.doi.org/10.1186/gb-2007-8-6-r118.

35. Pollard KS, Salama SR, King B, Kern AD, Dreszer T, Katzman S, et al. Forces shaping the fastest evolving regions in the human genome. PLoS Genet 2006; 2:e168; PMID:17040131; http://dx.doi.org/10.1371/journal.pgen.0020168.

36. Dreszer TR, Wall GD, Haussler D, Pollard KS. Biased clustered substitutions in the human genome: the footprints of male-driven biased gene conversion. Genome Res 2007; 17:1420-30; PMID:17785536; http://dx.doi.org/10.1101/gr.6395807.

37. Berglund J, Pollard KS, Webster MT. Hotspots of biased nucleotide substitutions in human genes. PLoS Biol 2009; 7:e26; PMID:19175294; http://dx.doi.org/10.1371/journal.pbio.1000026.

38. Katzman S, Kern AD, Pollard KS, Salama SR, Haussler D. GC-biased evolution near human accelerated regions. PLoS Genet 2010; 6:e1000960; PMID:20502635; http://dx.doi.org/10.1371/journal.pgen.1000960.

39. Ratnakumar A, Mousset S, Glémin S, Berglund J, Galtier N, Duret L, et al. Detecting positive selection within genomes: the problem of biased gene conversion. Philos Trans R Soc Lond B Biol Sci 2010; 365:2571-80; PMID:20643747; http://dx.doi.org/10.1098/rstb.2010.0007.

40. Galtier N, Duret L. Adaptation or biased gene conversion? Extending the null hypothesis of molecular evolution. Trends Genet 2007; 23:273-7; PMID:17418442; http://dx.doi.org/10.1016/j.tig.2007.03.011.

41. Cohen NM, Kenigsberg E, Tanay A. Primate CpG islands are maintained by heterogeneous evolutionary regimes involving minimal selection. Cell 2011; 145:773-86; PMID:21620139; http://dx.doi.org/10.1016/j.cell.2011.04.024.

42. Branciamore S, Chen ZX, Riggs AD, Rodin SN. CpG island clusters and pro-epigenetic selection for CpGs in protein-coding exons of HOX and other transcription factors. Proc Natl Acad Sci U S A 2010; 107:15485-90; PMID:20716685; http://dx.doi.org/10.1073/pnas.1010506107.

43. Chimpanzee Sequencing and Analysis Consortium. Initial sequence of the chimpanzee genome and comparison with the human genome. Nature 2005; 437:69-87; PMID:16136131; http://dx.doi.org/10.1038/nature04072.

44. Boffelli D, McAuliffe J, Ovcharenko D, Lewis KD, Ovcharenko I, Pachter L, et al. Phylogenetic shadowing of primate sequences to find functional regions of the human genome. Science 2003; 299:1391-4; PMID:12610304; http://dx.doi.org/10.1126/science.1081331.

45. Wang QF, Prabhakar S, Chanan S, Cheng JF, Rubin EM, Boffelli D. Detection of weakly conserved ancestral mammalian regulatory sequences by primate comparisons. Genome Biol 2007; 8:R1; PMID:17201929; http://dx.doi.org/10.1186/gb-2007-8-1-r1.

46. Kadonaga JT. Regulation of RNA polymerase II transcription by sequence-specific DNA binding factors. Cell 2004; 116:247-57; PMID:14744435; http://dx.doi.org/10.1016/S0092-8674(03)01078-X.

47. Hellman A, Chess A. Gene body-specific methylation on the active X chromosome. Science 2007; 315:1141-3; PMID:17322062; http://dx.doi.org/10.1126/science.1136352.

48. Suzuki MM, Bird A. DNA methylation landscapes: provocative insights from epigenomics. Nat Rev Genet 2008; 9:465-76; PMID:18463664; http://dx.doi.org/10.1038/nrg2341.

49. Chodavarapu RK, Feng S, Bernatavichute YV, Chen PY, Stroud H, Yu Y, et al. Relationship between nucleosome positioning and DNA methylation. Nature 2010; 466:388-92; PMID:20512117; http://dx.doi.org/10.1038/nature09147.

50. Schulz R, Proudhon C, Bestor TH, Woodfine K, Lin CS, Lin SP, et al. The parental non-equivalence of imprinting control regions during mammalian development and evolution. PLoS Genet 2010; 6:e1001214; PMID:21124941; http://dx.doi.org/10.1371/journal.pgen.1001214.

51. Paten B, Herrero J, Beal K, Fitzgerald S, Birney E. Enredo and Pecan: genome-wide mammalian consistency-based multiple alignment with paralogs. Genome Res 2008; 18:1814-28; PMID:18849524; http://dx.doi.org/10.1101/gr.076554.108.

52. Paten B, Herrero J, Fitzgerald S, Beal K, Flicek P, Holmes I, et al. Genome-wide nucleotide-level mammalian ancestor reconstruction. Genome Res 2008; 18:1829-43; PMID:18849525; http://dx.doi.org/10.1101/gr.076521.108.

53. Durbin RM, Abecasis GR, Altshuler DL, Auton A, Brooks LD, Gibbs RA, et al.; 1000 Genomes Project Consortium. A map of human genome variation from population-scale sequencing. Nature 2010; 467:1061-73; PMID:20981092; http://dx.doi.org/10.1038/nature09534.

54. Coop G, Wen X, Ober C, Pritchard JK, Przeworski M. High-resolution mapping of crossovers reveals extensive variation in fine-scale recombination patterns among humans. Science 2008; 319:1395-8; PMID:18239090; http://dx.doi.org/10.1126/science.1151851.

55. Sirmaci A, Spiliopoulos M, Brancati F, Powell E, Duman D, Abrams A, et al. Mutations in ANKRD11 cause KBG syndrome, characterized by intellectual disability, skeletal malformations, and macrodontia. Am J Hum Genet 2011; 89:289-94; PMID:21782149; http://dx.doi.org/10.1016/j.ajhg.2011.06.007.

56. Frints SG, Marynen P, Hartmann D, Fryns JP, Steyaert J, Schachner M, et al. CALL interrupted in a patient with non-specific mental retardation: gene dosage-dependent alteration of murine brain development and behavior. Hum Mol Genet 2003; 12:1463-74; PMID:12812975; http://dx.doi.org/10.1093/hmg/ddg165.

57. Kleefstra T, Brunner HG, Amiel J, Oudakker AR, Nillesen WM, Magee A, et al. Loss-of-function mutations in euchromatin histone methyl transferase 1 (EHMT1) cause the 9q34 subtelomeric deletion syndrome. Am J Hum Genet 2006; 79:370-7; PMID:16826528; http://dx.doi.org/10.1086/505693.

58. Boycott KM, Flavelle S, Bureau A, Glass HC, Fujiwara TM, Wirrell E, et al. Homozygous deletion of the very low density lipoprotein receptor gene causes autosomal recessive cerebellar hypoplasia with cerebral gyral simplification. Am J Hum Genet 2005; 77:477-83; PMID:16080122; http://dx.doi.org/10.1086/444400.

59. Trommsdorff M, Gotthardt M, Hiesberger T, Shelton J, Stockinger W, Nimpf J, et al. Reeler/Disabled-like disruption of neuronal migration in knockout mice lacking the VLDL receptor and ApoE receptor 2. Cell 1999; 97:689-701; PMID:10380922; http://dx.doi.org/10.1016/S0092-8674(00)80782-5.

60. Marshall CR, Noor A, Vincent JB, Lionel AC, Feuk L, Skaug J, et al. Structural variation of chromosomes in autism spectrum disorder. Am J Hum Genet 2008; 82:477-88; PMID:18252227; http://dx.doi.org/10.1016/j.ajhg.2007.12.009.

61. Pinto D, Pagnamenta AT, Klei L, Anney R, Merico D, Regan R, et al. Functional impact of global rare copy number variation in autism spectrum disorders. Nature 2010; 466:368-72; PMID:20531469; http://dx.doi.org/10.1038/nature09146.

62. Djurovic S, Gustafsson O, Mattingsdal M, Athanasiu L, Bjella T, Tesli M, et al. A genome-wide association study of bipolar disorder in Norwegian individuals, followed by replication in Icelandic sample. J Affect Disord 2010; 126:312-6; PMID:20451256; http://dx.doi.org/10.1016/j.jad.2010.04.007.

63. Poskanzer KE, Marek KW, Sweeney ST, Davis GW. Synaptotagmin I is necessary for compensatory synaptic vesicle endocytosis in vivo. Nature 2003; 426:559-63; PMID:14634669; http://dx.doi.org/10.1038/nature02184.

64. Seshadri S, DeStefano AL, Au R, Massaro JM, Beiser AS, Kelly-Hayes M, et al. Genetic correlates of brain aging on MRI and cognitive test measures: a genome-wide association and linkage analysis in the Framingham Study. BMC Med Genet 2007; 8(Suppl 1):S15; PMID:17903297; http://dx.doi.org/10.1186/1471-2350-8-S1-S15.

65. McLean CY, Bristor D, Hiller M, Clarke SL, Schaar BT, Lowe CB, et al. GREAT improves functional interpretation of cis-regulatory regions. Nat Biotechnol 2010; 28:495-501; PMID:20436461; http://dx.doi.org/10.1038/nbt.1630.

66. King MC, Wilson AC. Evolution at two levels in humans and chimpanzees. Science 1975; 188:107-16; PMID:1090005; http://dx.doi.org/10.1126/science.1090005.

67. Yu A, Zhao C, Fan Y, Jang W, Mungall AJ, Deloukas P, et al. Comparison of human genetic and sequence-based physical maps. Nature 2001; 409:951-3; PMID:11237020; http://dx.doi.org/10.1038/35057185.

68. Down TA, Rakyan VK, Turner DJ, Flicek P, Li H, Kulesha E, et al. A Bayesian deconvolution strategy for immunoprecipitation-based DNA methylome analysis. Nat Biotechnol 2008; 26:779-85; PMID:18612301; http://dx.doi.org/10.1038/nbt1414.

69. Illingworth R, Kerr A, Desousa D, Jørgensen H, Ellis P, Stalker J, et al. A novel CpG island set identifies tissue-specific methylation at developmental gene loci. PLoS Biol 2008; 6:e22; PMID:18232738; http://dx.doi.org/10.1371/journal.pbio.0060022.

70. Deaton AM, Webb S, Kerr AR, Illingworth RS, Guy J, Andrews R, et al. Cell type-specific DNA methylation at intragenic CpG islands in the immune system. Genome Res 2011; 21:1074-86; PMID:21628449; http://dx.doi.org/10.1101/gr.118703.110.

71. Wang H, Xing J, Grover D, Hedges DJ, Han K, Walker JA, et al. SVA elements: a hominid-specific retroposon family. J Mol Biol 2005; 354:994-1007; PMID:16288912; http://dx.doi.org/10.1016/j.jmb.2005.09.085.

72. Warnefors M, Pereira V, Eyre-Walker A. Transposable elements: insertion pattern and impact on gene expression evolution in hominids. Mol Biol Evol 2010; 27:1955-62; PMID:20332159; http://dx.doi.org/10.1093/molbev/msq084.

73. Cordaux R, Batzer MA. The impact of retrotransposons on human genome evolution. Nat Rev Genet 2009; 10:691-703; PMID:19763152; http://dx.doi.org/10.1038/nrg2640.

74. Khaitovich P, Hellmann I, Enard W, Nowick K, Leinweber M, Franz H, et al. Parallel patterns of evolution in the genomes and transcriptomes of humans and chimpanzees. Science 2005; 309:1850-4; PMID:16141373; http://dx.doi.org/10.1126/science.1108296.

75. Lienert F, Wirbelauer C, Som I, Dean A, Mohn F, Schübeler D. Identification of genetic elements that autonomously determine DNA methylation states. Nat Genet 2011; 43:1091-7; PMID:21964573; http://dx.doi.org/10.1038/ng.946.

76. Bock C, Walter J, Paulsen M, Lengauer T. CpG island mapping by epigenome prediction. PLoS Comput Biol 2007; 3:e110; PMID:17559301; http://dx.doi.org/10.1371/journal.pcbi.0030110.

77. Li Y, Zhu J, Tian G, Li N, Li Q, Ye M, et al. The DNA methylome of human peripheral blood mononuclear cells. PLoS Biol 2010; 8:e1000533; PMID:21085693; http://dx.doi.org/10.1371/journal.pbio.1000533.

78. Wu H, Caffo B, Jaffee HA, Irizarry RA, Feinberg AP. Redefining CpG islands using hidden Markov models. Biostatistics 2010; 11:499-514; PMID:20212320; http://dx.doi.org/10.1093/biostatistics/kxq005.

79. Lander ES. Initial impact of the sequencing of the human genome. Nature 2011; 470:187-97; PMID:21307931; http://dx.doi.org/10.1038/nature09792.

80. Wu DD, Irwin DM, Zhang YP. De novo origin of human protein-coding genes. PLoS Genet 2011; 7:e1002379; PMID:22102831; http://dx.doi.org/10.1371/journal.pgen.1002379.

81. Carroll SB. Evo-devo and an expanding evolutionary synthesis: a genetic theory of morphological evolution. Cell 2008; 134:25-36; PMID:18614008; http://dx.doi.org/10.1016/j.cell.2008.06.030.

82. McLean CY, Reno PL, Pollen AA, Bassan AI, Capellini TD, Guenther C, et al. Human-specific loss of regulatory DNA and the evolution of human-specific traits. Nature 2011; 471:216-9; PMID:21390129; http://dx.doi.org/10.1038/nature09774.

83. Robertson KD. DNA methylation and human disease. Nat Rev Genet 2005; 6:597-610; PMID:16136652; http://dx.doi.org/10.1038/nrg1655.

84. Shukla S, Kavak E, Gregory M, Imashimizu M, Shutinoski B, Kashlev M, et al. CTCF-promoted RNA polymerase II pausing links DNA methylation to splicing. Nature 2011; 479:74-9; PMID:21964334; http://dx.doi.org/10.1038/nature10442.

85. Somel M, Franz H, Yan Z, Lorenc A, Guo S, Giger T, et al. Transcriptional neoteny in the human brain. Proc Natl Acad Sci U S A 2009; 106:5743-8; PMID:19307592; http://dx.doi.org/10.1073/pnas.0900544106.

86. Illingworth RS, Gruenewald-Schneider U, Webb S, Kerr AR, James KD, Turner DJ, et al. Orphan CpG islands identify numerous conserved promoters in the mammalian genome. PLoS Genet 2010; 6:6; PMID:20885785; http://dx.doi.org/10.1371/journal.pgen.1001134.

87. Johnson LJ, Tricker PJ. Epigenomic plasticity within populations: its evolutionary significance and potential. Heredity (Edinb) 2010; 105:113-21; PMID:20332811; http://dx.doi.org/10.1038/hdy.2010.25.

88. Carbone L, Harris RA, Vessere GM, Mootnick AR, Humphray S, Rogers J, et al. Evolutionary breakpoints in the gibbon suggest association between cytosine methylation and karyotype evolution. PLoS Genet 2009; 5:e1000538; PMID:19557196; http://dx.doi.org/10.1371/journal.pgen.1000538.

89. Wilkinson LS, Davies W, Isles AR. Genomic imprinting effects on brain development and function. Nat Rev Neurosci 2007; 8:832-43; PMID:17925812; http://dx.doi.org/10.1038/nrn2235.

90. Gregg C, Zhang J, Butler JE, Haig D, Dulac C. Sex-specific parent-of-origin allelic expression in the mouse brain. Science 2010; 329:682-5; PMID:20616234; http://dx.doi.org/10.1126/science.1190831.

91. Iwamoto K, Bundo M, Ueda J, Oldham MC, Ukai W, Hashimoto E, et al. Neurons show distinctive DNA methylation profile and higher interindividual variations compared with non-neurons. Genome Res 2011; 21:688-96; PMID:21467265; http://dx.doi.org/10.1101/gr.112755.110.

92. Schroeder DI, Lott P, Korf I, LaSalle JM. Large-scale methylation domains mark a functional subset of neuronally expressed genes. Genome Res 2011; 21:1583-91; PMID:21784875; http://dx.doi.org/10.1101/gr.119131.110.

93. Levenson JM, Roth TL, Lubin FD, Miller CA, Huang IC, Desai P, et al. Evidence that DNA (cytosine-5) methyltransferase regulates synaptic plasticity in the hippocampus. J Biol Chem 2006; 281:15763-73; PMID:16606618; http://dx.doi.org/10.1074/jbc.M511767200.

94. McGraw CM, Samaco RC, Zoghbi HY. Adult neural function requires MeCP2. Science 2011; 333:186; PMID:21636743; http://dx.doi.org/10.1126/science.1206593.

95. Talkowski ME, Mullegama SV, Rosenfeld JA, van Bon BW, Shen Y, Repnikova EA, et al. Assessment of 2q23.1 microdeletion syndrome implicates MBD5 as a single causal locus of intellectual disability, epilepsy, and autism spectrum disorder. Am J Hum Genet 2011; 89:551-63; PMID:21981781; http://dx.doi.org/10.1016/j.ajhg.2011.09.011.

96. Arnheim N, Calabrese P. Understanding what determines the frequency and pattern of human germline mutations. Nat Rev Genet 2009; 10:478-88; PMID:19488047; http://dx.doi.org/10.1038/nrg2529.

97. Winckler W, Myers SR, Richter DJ, Onofrio RC, McDonald GJ, Bontrop RE, et al. Comparison of fine-scale recombination rates in humans and chimpanzees. Science 2005; 308:107-11; PMID:15705809; http://dx.doi.org/10.1126/science.1105322.

98. Baudat F, Buard J, Grey C, Fledel-Alon A, Ober C, Przeworski M, et al. PRDM9 is a major determinant of meiotic recombination hotspots in humans and mice. Science 2010; 327:836-40; PMID:20044539; http://dx.doi.org/10.1126/science.1183439.

99. Oliver PL, Goodstadt L, Bayes JJ, Birtle Z, Roach KC, Phadnis N, et al. Accelerated evolution of the Prdm9 speciation gene across diverse metazoan taxa. PLoS Genet 2009; 5:e1000753; PMID:19997497; http://dx.doi.org/10.1371/journal.pgen.1000753.

100. Frankel N, Erezyilmaz DF, McGregor AP, Wang S, Payre F, Stern DL. Morphological evolution caused by many subtle-effect substitutions in regulatory DNA. Nature 2011; 474:598-603; PMID:21720363; http://dx.doi.org/10.1038/nature10200.

101. Crespi BJ. The origins and evolution of genetic disease risk in modern humans. Ann N Y Acad Sci 2010; 1206:80-109; PMID:20860684; http://dx.doi.org/10.1111/j.1749-6632.2010.05707.x.

102. Molaro A, Hodges E, Fang F, Song Q, McCombie WR, Hannon GJ, et al. Sperm methylation profiles reveal features of epigenetic inheritance and evolution in primates. Cell 2011; 146:1029-41; PMID:21925323; http://dx.doi.org/10.1016/j.cell.2011.08.016.

103. Martin DI, Singer M, Dhahbi J, Mao G, Zhang L, Schroth GP, et al. Phyloepigenomic comparison of great apes reveals a correlation between somatic and germline methylation states. Genome Res 2011; 21:2049-57; PMID:21908772; http://dx.doi.org/10.1101/gr.122721.111.

104. Baillie JK, Barnett MW, Upton KR, Gerhardt DJ, Richmond TA, De Sapio F, et al. Somatic retrotransposition alters the genetic landscape of the human brain. Nature 2011; 479:534-7; PMID:22037309; http://dx.doi.org/10.1038/nature10531.

105. Conrad DF, Keebler JE, DePristo MA, Lindsay SJ, Zhang Y, Casals F, et al.; 1000 Genomes Project. Variation in genome-wide mutation rates within and between human families. Nat Genet 2011; 43:712-4; PMID:21666693; http://dx.doi.org/10.1038/ng.862.

106. Schmidt D, Wilson MD, Ballester B, Schwalie PC, Brown GD, Marshall A, et al. Five-vertebrate ChIP-seq reveals the evolutionary dynamics of transcription factor binding. Science 2010; 328:1036-40; PMID:20378774; http://dx.doi.org/10.1126/science.1186176.

107. Gojobori J, Tang H, Akey JM, Wu CI. Adaptive evolution in humans revealed by the negative correlation between the polymorphism and fixation phases of evolution. Proc Natl Acad Sci U S A 2007; 104:3907-12; PMID:17360451; http://dx.doi.org/10.1073/pnas.0605565104.

108. Jiang C, Zhao Z. Directionality of point mutation and 5-methylcytosine deamination rates in the chimpanzee genome. BMC Genomics 2006; 7:316; PMID:17166280; http://dx.doi.org/10.1186/1471-2164-7-316.

109. Mills RE, Walter K, Stewart C, Handsaker RE, Chen K, Alkan C, et al.; 1000 Genomes Project. Mapping copy number variation by population-scale genome sequencing. Nature 2011; 470:59-65; PMID:21293372; http://dx.doi.org/10.1038/nature09708.

110. Butcher LM, Beck S. AutoMeDIP-seq: a high-throughput, whole genome, DNA methylation assay. Methods 2010; 52:223-31; PMID:20385236; http://dx.doi.org/10.1016/j.ymeth.2010.04.003.

111. Wilson G, Dhami P, Feber A, Cortazar D, Suzuki Y, Schulz R, et al. Resources for methylome analysis suitable for gene knockout studies of potential epigenome modifiers. GigaScience 2012; 1:3; http://dx.doi.org/10.1186/2047-217X-1-3.

112. Li H, Durbin R. Fast and accurate short read alignment with Burrows-Wheeler transform. Bioinformatics 2009; 25:1754-60; PMID:19451168; http://dx.doi.org/10.1093/bioinformatics/btp324.

113. Li H, Handsaker B, Wysoker A, Fennell T, Ruan J, Homer N, et al.; 1000 Genome Project Data Processing Subgroup. The Sequence Alignment/Map format and SAMtools. Bioinformatics 2009; 25:2078-9; PMID:19505943; http://dx.doi.org/10.1093/bioinformatics/btp352.

114. Gentleman RC, Carey VJ, Bates DM, Bolstad B, Dettling M, Dudoit S, et al. Bioconductor: open software development for computational biology and bioinformatics. Genome Biol 2004; 5:R80; PMID:15461798; http://dx.doi.org/10.1186/gb-2004-5-10-r80.

115. Chavez L, Jozefczuk J, Grimm C, Dietrich J, Timmermann B, Lehrach H, et al. Computational analysis of genome-wide DNA methylation during the differentiation of human embryonic stem cells along the endodermal lineage. Genome Res 2010; 20:1441-50; PMID:20802089; http://dx.doi.org/10.1101/gr.110114.110.

116. Fujita PA, Rhead B, Zweig AS, Hinrichs AS, Karolchik D, Cline MS, et al. The UCSC Genome Browser database: update 2011. Nucleic Acids Res 2011; 39(Database issue):D876-82; PMID:20959295; http://dx.doi.org/10.1093/nar/gkq963.

117. Ihaka R, Gentleman RR. A Language for Data Analysis and Graphics. J Comput Graph Statist 1996; 5:299-314.